Nonlinear Dyn (2021) 104:2621–2638
https://doi.org/10.1007/s11071-021-06421-3

ORIGINAL PAPER

# Dynamic behaviors of general $N$-solitons for the nonlocal generalized nonlinear Schrödinger equation

**Minmin Wang · Yong Chen**

Received: 4 December 2020 / Accepted: 29 March 2021 / Published online: 11 May 2021


**Abstract** The general $N$-solitons of nonlocal generalized nonlinear Schrödinger equations with third-order, fourth-order and fifth-order dispersion terms and nonlinear terms (NGNLS) are studied. Firstly, the Riemann–Hilbert problem and the general $N$-soliton solutions of NGNLS equations were given. Then, we study the symmetry relations of the eigenvalues and eigenvectors related to the scattering data which involve the reverse-space, reverse-time and reverse-space-time reductions. Thirdly, some novel solitons and the dynamic behaviors which corresponded to novel eigenvalue configurations and the coefficients of higher-order terms are given. In all the three NGNLS equations, their solutions often collapse periodically, but can remain bounded or nonsingular for wide ranges of soliton parameters as well. In addition, it is found that the higher-order terms of the NGNLS equations not only affect the amplitude variation of the soliton, but also influence the singularity and the motion of the soliton.

**Keywords** Nonlocal generalized nonlinear Schrödinger equation · Riemann–Hilbert method · General $N$-soliton solutions

The project is supported by National Natural Science Foundation of China (No. 11675054), Science and Technology Commission of Shanghai Municipality (No. 18dz2271000) and Future Scientist and Outstanding Scholar Cultivation Program of East China Normal University (No.WLKXJ202001).

M. Wang · Y. Chen
School of Mathematical Sciences, Shanghai Key Laboratory of PMMP, Shanghai Key Laboratory of PMMP, Shanghai Key Laboratory of Trustworthy Computing, East China Normal University, Shanghai 200062, P. R. China

Y. Chen (✉)
College of Mathematics and Systems Science, Shandong University of Science and Technology, Qingdao 266590, P. R. China
e-mail: profchenyong@163.com

Y. Chen
Department of Physics, Zhejiang Normal University, Jinhua 321004, P. R. China

## 1 Introduction

Inverse scattering transformation (IST) method was first proposed by Garder, Greene, Kruskal and Miura in 1967 [1]. The origin of the soliton theory was first introduced by utilizing inverse scattering method to solve the nonlinear partial differential equation with initial value conditions. Then in 1972, Zakharov and Shabat first solved the initial value problem for the classical nonlinear Schrödinger equation (NLS) by IST method [2]. IST method [3] started from the linear problem which is corresponded to the equation; then combining the translation transformation and scattering data, the problem was converted into solving an integral Gelfand–Levitan–Marchenko (GLM) equation [4]. However, solving the corresponding integral GLM equation is a very cumbersome process. Then, a more direct method: Riemann–Hilbert problem (RHP) method, was introduced to replace the GLM integral equations [5]. With the help of RHP, the solving process is greatly simplified rather than based on the GLM integral equation. RHP method was first used to get soliton solutions of the NLS equation in 1984 by Zakharov et. al [6], which is the modern version of RHP method. From then on, RHP method began to become popular and there are a growing number of advances in solving soliton solutions by RHP method [10–14].

Parity-time (PT) symmetry plays a vital role in the spectrum of the Hamiltonian, Bender and Boettcher [7] proved that a wide class of non-Hermitian Hamiltonians with PT symmetry have real and positive spectrum. Then, a new integrable nonlocal NLS equation is introduced by Ablowitz and Musslimani [8], where they discuss the IST and scattering data with suitable symmetries and they found an explicit breathing one-soliton solution and then developed the inverse scattering theory by using a novel left–right RHP and presented the explicit time-periodic one and two-soliton solutions [9]. Then, a lot of nonlocal systems have been researched by [15–18], and by Darboux transformation, a variety of solutions were obtained [19–22]. However, the previous research work only obtained the basic soliton solution for the local system. The multi-soliton solutions by Riemann–Hilbert problem for the local system have been extensively explored in many papers. There are not many studies on multi-soliton solutions of nonlocal system by RHP method. In 2018, Yang [23] obtained some new soliton solutions of the nonlocal NLS equation by RHP method and found that multi-soliton solutions can behave very differently from fundamental solitons and may not correspond to a nonlinear superposition of fundamental solitons. Besides, in addition to solitons of the reverse-space NLS equation, Yang also obtained the solitons of the reverse-time and reverse-space-time NLS equation which have not been discussed in the previous work. In the framework of IST and RHP, we can clearly see the novel symmetry relations in their scattering data, which is completely different from those in the corresponding local NLS equation.

The standard NLS equation is a physics approximation of the evolution of waves in various systems. To realize a more realistic approximation of the additional phenomena in real physical system, the effects of higher-order terms had to been taken into consideration, such as the self-steepening, self-frequency shift and high-order dispersion [24–27]. Among them, with increasing intensity of the optical field and further shortening of pulses up to attosecond durations in a gas medium [25], the role of quintic terms is becoming ever more important. In 2014, Chowdury et al. considered a NLS equation with quintic terms [28], where they concluded a new soliton with new structure which cannot be exist for the standard NLS equation. The equation in [28] with local potential had been researched extensively and there have been many results. By Darboux transformation, the rogue waves, rational solitons and modulational instability of the fifth-order NLS equation in [28] had been studied by Yang in 2015 [32]. By Hirota method with two auxiliary functions, soliton solutions and interaction of the dark solitons are illustrated graphically in [33]. In [34], Several classes of $N$-solitons exhibiting elastic collisions and nonelastic collisions that lead to the gain and the loss of amplitudes after collision in a conservative system were presented. Then in 2018, they consider the higher-order rational solutions for a new nonlocal Eq. [35]. In this paper, we will explore the $N$-soliton solutions of the following coupled generalized NLS (GNLS) system in [28,35]

$$\begin{cases} q_t = F_1(q) + iF_2(q,r) + \alpha F_3(q,r) + i\gamma F_4(q,r) + \beta F_5(q,r), \\ r_t = G_1(r) - iG_2(q,r) + \alpha G_3(q,r) - i\gamma G_4(q,r) + \beta G_5(q,r) \end{cases} \tag{1}$$

where $q,\ r$ are complex functions of $(x,t)$ with their modulus representing the envelope of the waves, $\alpha,\ \gamma$ and $\delta$ are three arbitrary real parameters and $F_1(q)$ and $G_1(r)$ are the expressions as follows:

$$F_1(q) = -i\delta_1 q + \delta_2 q_x,\quad G_1(r) = i\delta_1 r + \delta_2 r_x$$

with $\delta_1$ and $\delta_2$ being arbitrary real parameters. The differential polynomial

$$F_2(q,r) = \tfrac{1}{2}q_{xx} + q^2 r$$

represents the NLS operator part beginning with the second-order dispersion.

$$F_3(q,r) = q_{xxx} + 6rqq_x$$

stands for the Hirota operator part beginning with the third-order dispersion.

$$F_4(q,r) = q_{xxxx} + 6r^2q^3 + 2q^2r_{xx} + 8qrq_{xx} + 4qq_xr_x + 6rq_x^2$$

denotes the Lakshmanan–Porsezian–Daniel (LPD) operator part beginning with the fourth-order dispersion.

$$F_5(q,r) = q_{xxxxx} + 10qrq_{xxx} + 30q^2r^2q_x + 20rq_xq_{xx} + 10(qr_xq_x)_x$$

is the quintic operator part beginning with the fifth-order dispersion. Besides, $G_k(q, r)(k = 2, 3, 4, 5)$ are expressions after swapping $q$ and $r$ in $F_k(q, r)(k = 2, 3, 4, 5)$.

Since the corresponding terms $q$, $r$ and its first-order derivative in $F_1$ and $G_1$ are relevant phase and velocity transformations, the parameters $\delta_1, \delta_2$ are regarded as zeros here. For convenience, resign the parameters $\alpha$, $\beta$ and $\gamma$ as an array $C$, i.e., $C = \left[\alpha,\ \gamma,\ \beta\right]$. When $C = [0,\ 0,\ 0]$, the system (1) reduces to the coupled standard NLS system. The coupled Hirota system and LPD system can be obtained when $C$ take $[1,\ 0,\ 0]$ and $[0,\ 1,\ 0]$, respectively. In this paper, we will investigate the influence of the values of $C$ on the solution, especially when $\gamma \neq 0$.

The reverse-space GNLS equation

$$\begin{aligned} q_t(x,t) = {} & iF_2(q(x,t), q^*(-x,t)) \\ & +\alpha F_3(q(x,t), q^*(-x,t)) \\ & +i\gamma F_4(q(x,t), q^*(-x,t)) \\ & +\beta F_5(q(x,t), q^*(-x,t)), \end{aligned} \tag{2}$$

reverse-time GNLS equation

$$\begin{aligned} q_t(x,t) = {} & iF_2(q(x,t), -q(x,-t)) \\ & +\alpha F_3(q(x,t), -q(x,-t)) \\ & +i\gamma F_4(q(x,t), -q(x,-t)) \\ & +\beta F_5(q(x,t), -q(x,-t)), \end{aligned} \tag{3}$$

as well as the reverse-space-time GNLS equation

$$\begin{aligned} q_t(x,t) = {} & iF_2(q(x,t), q(-x,-t)) \\ & +\alpha F_3(q(x,t), q(-x,-t)) \\ & +i\gamma F_4(q(x,t), q(-x,-t)) \\ & +\beta F_5(q(x,t), q(-x,-t)) \end{aligned} \tag{4}$$

corresponding to the GNLS equation (1) can be obtained by the reverse-space reduction

$$r(x,t) = q^*(-x,t), \tag{5}$$

the reverse-time reduction

$$r(x,t) = -q(x,-t), \tag{6}$$

and the reverse-space-time reduction

$$r(x,t) = q(-x,-t). \tag{7}$$

For the three kinds of NGNLS equations (2), (3) and (4) above, there has been not much research on it as far as I know. Inspired by the interesting discussions in [23] of the novel solitons for the nonlocal NLS equations, we expect that these phenomena might be also valid for the NGNLS equations. In this paper, we will explore some new soliton solutions for the NGNLS equations (2), (3) and (4) above. We would like to be able to figure out the correspondence of new spectrum configurations and the solitons of new shapes when the potential function under reduction (5), (6) and (7). Besides, we will focus on the physical effects corresponding to the higher-order terms which involve Hirota part, LPD part and the quintic part, especially the quintic part, i.e., the value of $C$ is essential, and in what follows, we will investigate this influence of the higher-order terms on the structures of $N$-soliton solutions.

The structures of this work are as follows. At first, the introduction mainly concerns the backgrounds and the motivations. Then, we give the RHP for Eq.(1) in Sect. 2. Then, we study the symmetry relations of the scattering data and conclude the $N$-soliton solutions for NGNLS (2), (3) and (4) in Sect. 3. In Sect. 4, some novel soliton solutions and bound-state solitons are given, and the corresponding dynamic behaviors of the solitons for the NGNLS equations (2), (3) and (4) are analyzed. The last section is the conclusion.

## 2 The Riemann–Hilbert problem

The Riemann–Hilbert problem and the $N$-soliton formula of the NLS system have been considered in [10]. But system (1) has a quite different time evolution and contains the effects of the higher-order terms. In this section, we will give the corresponding $N$-soliton formula for system (1) when the potential matrix $Q$ decays to zero.

The lax pair for (1) is

$$\begin{cases} \Phi_x = (i\lambda\Sigma + iQ)\ \Phi, \\ \Phi_t = (if(\lambda)\Sigma + V)\ \Phi, \end{cases} \tag{8}$$

where $f(\lambda) = 16\beta\lambda^5 - 8\gamma\lambda^4 - 4\alpha\lambda^3 + \lambda^2 + \delta_2\lambda + \frac{1}{2}\delta_1$, $\Sigma = diag(1, -1)$,

$$Q = \begin{bmatrix} 0 & r \\ q & 0 \end{bmatrix},\ V = \sum_{j=0}^{4} \lambda^j V_j, \tag{9}$$

with $V_j$ $(j = 0, 1, 2, 3, 4)$ being polynomials of the potential matrix $Q$ and its derivative

$$\begin{aligned} & V_4 = 16i\beta Q, \\ & V_3 = i(-8\gamma Q + 8i\beta Q_x\Sigma - 8\beta Q^2)\Sigma, \\ & V_2 = 4i\gamma Q^2\Sigma - 4\beta(-QQ_x + Q_xQ) + 8\gamma \\ & \qquad Q_x\Sigma - 4iQ\alpha - 4i\beta Q_{xx} - 4\gamma Q_x\Sigma - 8i\beta Q^3, \end{aligned}$$

$$
\begin{aligned}
V_1 = i\Big[&2\alpha Q^2\Sigma + 6\beta Q^4\Sigma - 2i\gamma \\
&(-QQ_x + Q_xQ) + 2\beta(QQ_{xx} + Q_{xx}Q - Q_x^2)\Sigma + Q \\
&+4\gamma Q^3 - 2i\alpha Q_x\Sigma - 12i\beta \\
&Q^2Q_x\Sigma + 2\gamma Q_{xx} - 2i\beta Q_{xxx}\Sigma\Big], \\
V_0 = i\Big[&-\frac{1}{2}QQ\Sigma - 3\gamma Q^4\Sigma - i\alpha \\
&(-QQ_x + Q_xQ) - \gamma(QQ_{xx} + Q_{xx}Q - Q_x^2)\Sigma \\
&-6i\beta(Q_xQ^3 - Q^3Q_x) - i\beta(Q_{xxx} \\
&Q - QQ_{xxx} - Q_{xx}Q_x + Q_xQ_{xx}) + \delta_2 Q \\
&+2\alpha Q^3 + 6\beta Q^5 + \frac{1}{2}iQ_x\Sigma + 6i\gamma Q^2Q_x \\
&\Sigma + \alpha Q_{xx} + \beta(2QQ_{xx}Q + 4Q_xQ_xQ \\
&+6Q_xQQ_x + 8Q_{xx}Q^2) + i\gamma Q_{xxx}\Sigma + \beta Q_{xxxx}\Big]. \qquad (10)
\end{aligned}
$$

The system (1) can be produced by the zero-curvature equation with the Lax pair (8) above. The Lax pair was first introduced by Chowdury et. al. [28] in 2014. In [28], the elements of the matrix $V$ and $V_i$ are expressed as functions of the potential function $q$, $r$ and their derivatives. For the convenience of the analysis below, here we rewrite $V_i$ as more compact forms generated by the matrix $Q$ and its derivatives. And we have verified the expressions of $V_i$ are well defined.

In this work, our analysis is based on the initial condition

$$q(x,0), r(x,0) \in \mathbb{S}(\mathbb{R}), x \to \pm\infty. \qquad (11)$$

where $\mathbb{S}(\mathbb{R})$ represents the Schwartz space

$$\mathbb{S}(\mathbb{R}) = \left\{ s \in C^{\infty}(\mathbb{R}), \|s\|_{\alpha,\beta} = \sup_{x\in\mathbb{R}} \left|x^{\alpha}\partial^{\beta}s(x)\right| < \infty, \quad \alpha,\beta \in \mathbb{Z}_+ \right\}.$$

so the initial values of $q, r$ at $t = 0$ decay to zero sufficiently fast as $x \to \pm\infty$, i.e.,

$$q(x,0) \to 0, r(x,0) \to 0, x \to \pm\infty. \qquad (12)$$

Thus, when $x \to \pm\infty$, the potential matrix $Q$ and the matrix $V$ which is a function of $Q$ and the derivative of $Q$ all reduced to zero matrix quickly. Since the corresponding terms of $\delta_1$ and $\delta_2$ are related to the phase and velocity transformations of the solutions, in this paper, we take $\delta_1 = \delta_2 = 0$.

For briefness, sign

$$\theta(\lambda) = \lambda x + (16\beta\lambda^5 - 8\gamma\lambda^4 - 4\alpha\lambda^3 + \lambda^2)t.$$

So, under the initial condition, we can conclude that $\Phi \propto e^{i\theta\Sigma}$ from Lax pair Eqs. (8). Express $\Phi$ as $\Phi = Je^{i\theta\Sigma}$. Insert it into the Lax pair Eqs. (8). Then,

$$J_x = i\lambda[\Sigma, J] - iQJ, \qquad (13)$$

$$J_t = if(\lambda)[\Sigma, J] + VJ. \qquad (14)$$

where $[\Sigma, J] = \Sigma J - J\Sigma$ is the commutator.

Hereinafter, we only consider the first space scattering Eq. (13) and take $t$ as a dummy variable. Introduce the matrix $J_{1,2}$ as the Jost solutions of Eq.(13)

$$\begin{aligned} &J_1 \to I, x \to +\infty, \\ &J_2 \to I, x \to -\infty \end{aligned} \qquad (15)$$

and sign

$$J_1E = \Omega = (\omega_1, \omega_2), \ J_2E = \Psi = (\psi_1, \psi_2), \qquad (16)$$

where $I$ is the $2 \times 2$ identity matrix and $E = e^{i\lambda\Sigma x}$. Since $\Omega$ and $\Psi$ are two matrix solutions of the same linear ordinary differential equation, there should be a matrix $S(\lambda)$ which is independent of $x$ that satisfies

$$\Omega = \Psi S(\lambda), \ \lambda \in \mathbb{R}, \qquad (17)$$

so $J_1 = J_2ESE^{-1}$ and by the Abel's identity and $tr(Q) = 0$, we have $det(J_{1,2})(x,\lambda) = det S(\lambda) = 1$ for any $x$ and $\lambda \in \mathbb{R}$.

Imposing the boundary conditions (15)), the scattering Eq. (13) for $J_{1,2}$ can be resigned as Volterra-type integral equations of the form

$$J_1 = I + \int_{-\infty}^{x} e^{i\lambda\Sigma(x-y)}Q(y)J_1(y,\lambda)e^{-i\lambda\Sigma(x-y)}dy, \qquad (18)$$

$$J_2 = I - \int_{x}^{+\infty} e^{i\lambda\Sigma(x-y)}Q(y)J_2(y,\lambda)e^{-i\lambda\Sigma(x-y)}dy. \qquad (19)$$

Expanding the element of the matrix, the first column of $J_1$ can be analytically extended to $\lambda \in \mathbb{C}_-$ and the second column of $J_1$ can be analytically extended to $\lambda \in \mathbb{C}_+$. Similarly, the first column of $J_2$ can be analytically extended to $\lambda \in \mathbb{C}_+$ and the other column of $J_2$ can be analytically extended to $\lambda \in \mathbb{C}_-$. Resign

$$\begin{aligned} J_1 &= (J_{1,1}^-, J_{1,2}^+), \\ J_2 &= (J_{2,1}^+, J_{2,2}^-), \end{aligned} \qquad (20)$$

where the superscript $\pm$ of $J_{j,k}^{\pm}(j = 1,2, \ k = 1,2)$ represents the analyticity on the upper or lower half of the $\lambda$ complex plane, the subscript $j$ is same as the subscript of $J_j(j = 1,2)$, and $k$ represents the $k-$column of the matrix $J_j(j = 1,2)$. Thus, introducing the Jost solution

$$\begin{aligned} P^+ = (J_{1,2}^+, J_{2,1}^+) &= J_1H_2 + J_2H_1 \\ &= J_1H_2 + J_1ES^{-1}E^{-1}H_1 \\ &= J_1E\begin{bmatrix} \hat{s}_{11} & 0 \\ \hat{s}_{21} & 1 \end{bmatrix}E^{-1} \end{aligned} \qquad (21)$$

is analytic in $\lambda \in \mathbb{C}_+$ and

$$R^- = (J_{1,1}^-, J_{2,2}^-) = J_1H_1 + J_2H_2 \qquad (22)$$

is analytic in $\lambda \in \mathbb{C}_-$, where $H_1 = diag(1,0)$ and $H_2 = diag(0,1)$.

Implement the limit $\lambda \to \infty$ on the Volterra integral Eqs. (18), and we can get the large-$\lambda$ asymptotic

$$P^+(x,\lambda) \to I, \ \lambda \in \mathbb{C}_+ \to \infty. \tag{23}$$

By direct calculation, we can get that $\det(P^+) = \hat{s}_{11}$.

Considering the adjoint eigenvalue problem of equation (13)

$$K_x = i\lambda[\Sigma, K] + iKQ, \tag{24}$$

we can notice that $J_j^{-1}(j=1,2)$ satisfy Eq. (24). Combining (16) and taking the notations

$$\Omega^{-1} = \hat{\Omega} = (\hat{\omega}_1, \hat{\omega}_2)^T, \quad \Psi^{-1} = \hat{\Psi} = \left(\hat{\psi}_1, \hat{\psi}_2\right)^T, \tag{25}$$

then we can conclude that the first row of $J_1^{-1}$and the second rows of $J_2^{-1}$ are analytic in $\lambda \in \mathbb{C}_+$. Besides, the second row of $J_1^{-1}$ and the first row of $J_2^{-1}$ are analytic in $\lambda \in \mathbb{C}_-$, i.e.,

$$\begin{aligned} J_1^{-1} &= E\hat{\Omega} = \hat{J}_1 = (\hat{J}_{1,1}^+, \hat{J}_{1,2}^-)^T, \\ J_2^{-1} &= E\hat{\Psi} = \hat{J}_2 = (\hat{J}_{2,1}^-, \hat{J}_{2,2}^+)^T, \end{aligned} \tag{26}$$

where the superscript $\pm$ and the subscript $j,k$ of $\hat{J}_{j,k}^{\pm}(j=1,2,\ k=1,2)$ represent the same messages as in $J_{j,k}^{\pm}(j=1,2,\ k=1,2)$. So, the adjoint Jost solution can be constructed as

$$\begin{aligned} P^- = \left(\hat{J}_{1,2}^-, \hat{J}_{2,1}^-\right)^T &= H_2 J_1^{-1} + H_1 J_2^{-1} \\ &= H_2 J_1^{-1} + H_1 ESE^{-1} J_1^{-1} \\ &= E \begin{bmatrix} s_{11} & s_{21} \\ 0 & 1 \end{bmatrix} E^{-1} J_1^{-1}, \end{aligned} \tag{27}$$

the large $\lambda$-asymptotic behavior is

$$P^- \to I, \lambda \in \mathbb{C}_- \to \infty$$

and the determinant

$$\det(P^-) = s_{11}.$$

Similarly, we can see that the Jost solution $R^+ = H_1 J_1^{-1} + H_2 J_2^{-1} \to I, \lambda \in \mathbb{C}_+ \to \infty$ is analytic in $\lambda \in \mathbb{C}_+$.

In conclusion, the analytical properties of the Jost solutions can be shown as

$$\begin{aligned} \Omega &= \left(\omega_1^-, \omega_2^+\right), \quad \Omega^{-1} = \left(\hat{\omega}_1^+, \hat{\omega}_2^-\right)^T, \\ \Psi &= \left(\psi_1^+, \psi_2^-\right), \quad \Psi^{-1} = \left(\hat{\psi}_1^-, \hat{\psi}_2^+\right)^T \end{aligned} \tag{28}$$

and by Eq. (17), the analytical properties of the scattering matrix can be obtained

$$S^{-1} = \Omega^{-1}\Psi = \begin{pmatrix} \hat{s}_{11}^+ & \hat{s}_{12} \\ \hat{s}_{21} & \hat{s}_{22}^- \end{pmatrix}, \quad S = \begin{pmatrix} s_{11}^- & s_{12} \\ s_{21} & s_{22}^+ \end{pmatrix}, \tag{29}$$

where the superscript $\pm$ represents the analytical properties on the complex $\lambda$-plane. So, the RHP of the spectral Eq. (13) can be constructed as follows:

**Riemann-Hilbert Problem 1** *For $(x,t) \in R^2$, solve the find a $2\times 2$ matrix-valued function $P(x,t,\lambda)$ in the complex $\lambda$–plane such that*

- *The matrix function $P^+ = J_1 H_2 + J_2 H_1$ is analytic in $\lambda \in C_+$ and $P^- = H_2 J_1^{-1} + H_1 J_2^{-1}$ is analytic in $\lambda \in C_-$.*
- *The RHP*

$$P^-(x,\lambda)P^+(x,\lambda) = G(x,\lambda), \lambda \in \mathbb{R} \tag{30}$$

*is well defined on the real line, where the jump matrix can be obtained by (21) and (27) as*

$$G(x,\lambda) = E\begin{pmatrix} 1 & s_{12} \\ \hat{s_{21}} & 1 \end{pmatrix} E^{-1}.$$

- *The canonical normalization condition is $P^{\pm} \to I$ as $\lambda \to \infty$.*

It can be concluded by the previous analysis that $P^{\pm}$ are the matrix solutions of the scattering Eq. (13) and the adjoint scattering Eq. (24), respectively. Take the following expansions in (13) and (24) $P^{\pm} = I + \lambda^{-1}P_1^{\pm} + O(\lambda^{-2}), \lambda \to \infty$, and collect the same power of $\lambda^0$

$$Q = -\left[\Sigma, P_1^+\right] = \left[\Sigma, P_1^-\right], \tag{31}$$

Thus, the potential function $q$ and $r$ can be represented as

$$q = 2[P_1^+]_{21}, r = -2[P_1^+]_{12}. \tag{32}$$

In order to get $q$ and $r$, we just need to get the $P_1^+$; in the next section, we need to solve $P^+$ and $P^-$ from the RHP (30).

## 3 Solution to the RHP and the symmetry relations

In this section, we will discuss the solution to the RHP 1. Besides, we will give the corresponding symmetry relations under three different nonlocal reduction (5), (6) and (7).

### 3.1 Solution to the RHP 1

Firstly, we begin from $\det(P^+) \neq 0$, i.e., the RHP 1 is regular; under this circumstance, the matrix solution $P^+$ is nonsingular, so Eq. (30) can be rewritten as

$$(P^+)^{-1} - P^- = \hat{G}(P^+)^{-1}(\lambda), \tag{33}$$

where

$$\hat{G} = I - G = E\begin{bmatrix} 0 & s_{12} \\ \hat{s}_{21} & 0 \end{bmatrix} E^{-1}.$$

Utilizing the Plemelj formula and the canonical boundary condition and then implementing the similar process in [10], the unique solution to this regular RHP (33) takes the following form

$$(P^+)^{-1} = I + \frac{1}{2\pi i}\int_{-\infty}^{\infty}\frac{\hat{G}(P^+)^{-1}(\lambda)}{\zeta}. \qquad (34)$$

But in most cases, $\det(P^+)$ and $\det(P^-)$ are zeros at $\lambda_k \in \mathbb{C}^+$ and $\bar{\lambda}_k \in \mathbb{C}^-$, i.e., the RHP (30) is nonregular. We consider the simple zeros here. Suppose $\det(P^+)$ has $N$ simple zeros $\lambda_j (j = 1\ldots, N)$ in $\mathbb{C}^+$ and $\det(P^-)$ has $N$ simple zeros $\bar{\lambda}_j (j = 1\ldots, N)$ in $\mathbb{C}^-$, $v_j$ and $\bar{v}_j$ are the corresponding nonzero column and row vectors, i.e., $v_j$ and $\bar{v}_j$ are the solutions of the following equations

$$P^+(\lambda_j)v_j(\lambda_j) = 0, \qquad (35)$$

$$\bar{v}_j(\bar{\lambda}_j)P^- = 0. \qquad (36)$$

By Theorem 2.1 in [29], the solution of the nonregular RHP can be represented by the solution of the regular RHP, where the solution contains the integral part; when $G = I$, the scattering data are zero and the scattering process is reflectionless.

**Theorem 1** *The N-soliton solutions of system* (1) *can be written as*

$$q(x,t) = -2\frac{\det M_1}{\det M},\ r(x,t) = 2\frac{\det M_2}{\det M}, \qquad (37)$$

*where $M_1$ and $M_2$ are the $(N+1)\times(N+1)$ matrices as follows:*

$$M_1 = \begin{bmatrix} 0 & b_1e^{-\theta_1} & \ldots & b_Ne^{-\theta_N} \\ \bar{a}_1e^{\bar{\theta}_1} & m_{11} & \ldots & m_{1N} \\ \vdots & \vdots & \vdots & \vdots \\ \bar{a}_Ne^{\bar{\theta}_N} & m_{N1} & \ldots & m_{NN} \end{bmatrix},$$
$$M_2 = \begin{bmatrix} 0 & a_1e^{\theta_1} & \ldots & a_Ne^{\theta_N} \\ \bar{b}_1e^{-\bar{\theta}_1} & m_{11} & \ldots & m_{1N} \\ \vdots & \vdots & \vdots & \vdots \\ \bar{b}_Ne^{-\bar{\theta}_N} & m_{N1} & \ldots & m_{NN} \end{bmatrix}. \qquad (38)$$

*where $\theta_k = \lambda_k x + f(\lambda_k)t$ and $\bar{\theta}_k = -\bar{\lambda}_k x - f(\bar{\lambda}_k)t$, $a_k,\ b_k,\ \bar{a}_j,\ \bar{b}_j$ are arbitrary complex constants.*

If the scattering process is reflectionless, combining the formula (32), the so-called $N$-soliton formulas of system (1) can be written as

$$q(x,t) = 2\left(\sum_{j,k=1}^{N} v_j(M^{-1})_{jk}\bar{v}_k\right)_{21}, \qquad (39)$$

$$r(x,t) = -2\left(\sum_{j,k=1}^{N} v_j(M^{-1})_{jk}\bar{v}_k\right)_{12}, \qquad (40)$$

where $M$ is a $N\times N$ matrix, $(M^{-1})_{jk}$ is the element of the inverse matrix of $M$. The $(j,k)$-th element of $M$ is $m_{jk}(j,k = 1,2,\ldots,N)$ with

$$m_{jk} = \frac{\bar{v}_j v_k}{\bar{\lambda}_j - \lambda_k},\ j,k = 1,2,\ldots,N, \qquad (41)$$

where $\lambda_k, \bar{\lambda}_j$ are spectral parameters of the original problem and the adjoint problem, respectively. $v_k$ and $\bar{v}_k$ are column vector and row vector of length two. Recall Eqs. (35) and (36) and take the derivative of $x$ and $t$, respectively. Combining the Lax pair (13)-(14), we can get that

$$v_j = e^{i\theta_k\Sigma}v_{k_0},\quad \bar{v}_j = \bar{v}_{j0}e^{-i\bar{\theta}_j\Sigma} \qquad (42)$$

where $v_{k_0} = [a_k, b_k]$ and $\bar{v}_{j0} = \left[\bar{a}_j, \bar{b}_j\right]^T$ are two constant vectors with $a_k,\ b_k,\ \bar{a}_j,\ \bar{b}_j$ are complex constants.

*Remark* Similar to the determinant representation technique in [31] and [30], the $N$-soliton solutions (39) and (40) can be rewritten as the determination form (37).

## 3.2 Symmetry relation for the NGNLS equations

Under different nonlocal reductions (5), (6) and (7), the eigenvalues and eigenvectors satisfy different symmetry relations. In this section, we will investigate the symmetry relations of the scattering data, the eigenvalues and the corresponding eigenvectors for the three NGNLS equations (2), (3) and (4). For simplicity, denoting $\lambda_k = \xi_k + i\eta_k$ and $\bar{\lambda}_k = \bar{\xi}_k + i\bar{\eta}_k$, $k = 1,2,\ldots,N$, where $\xi_k, \bar{\xi}_k$ and $\eta_k, \bar{\eta}_k$ are the real and imaginary parts of $\lambda_k$ and $\bar{\lambda}_k$.

The potential matrix $Q(x,t)$ has the following initial condition:

$$Q_0 := Q(x,0) = \begin{pmatrix} 0 & r(x,0) \\ q(x,0) & 0 \end{pmatrix},$$

where $q(x,0), r(x,0)$ are the initial value of functions $q(x,t)$ and $r(x,t)$ at $t = 0$. Considering the eigenvalue problem

$$J_x = i\lambda[\Sigma, J] - iQ_0J,$$

and its adjoint eigenvalue problem

$$K_x = i\lambda[\Sigma, K] + iKQ_0.$$

Here, the eigenvalue problem (13) and (24) are different from which in [23] and with some complicated proofs, we get the following theorems.

**Theorem 2** *For the reverse-space NGNLS equation (2), the eigenvalues appear in pairs* $(\lambda_k, -\lambda_k^*)$.

1. *For the eigenvalue* $\lambda_k = \xi_k + i\eta_k$ *of the scattering equation (13) in* $\mathbb{C}_+$, *i.e.,* $\eta_k > 0$ *and* $\xi_k \in \mathbb{R}$, *we consider the following two cases:*

(1). *If* $\xi_k \neq 0$, *then* $\hat{\lambda} = -\lambda_k^*$ *is also the eigenvalue for the scattering equation (13) and the corresponding parameters in* $v_{k_0} = [a_k, b_k]$ *and* $\hat{v}_{k_0} = [\hat{a}_k, \hat{b}_k]$ *satisfy* $\hat{a}_k = b_k^*,\ \hat{b}_k = a_k^*$.

(2). *If* $\xi_k = 0$, *then* $\lambda_k = -\lambda_k^*$, *so the corresponding eigenvectors are* $v_{k_0} = [1, e^{i\theta_k}]$.

2. *For the eigenvalue* $\bar{\lambda}_k = \bar{\xi}_k - i\bar{\eta}_k$ *of the scattering equation (24) in* $\mathbb{C}_-$, *i.e.,* $\bar{\eta}_k > 0$ *and* $\bar{\xi}_k$ *is any real constant, we consider the following two cases:*

(1). *If* $\bar{\xi}_k \neq 0$, *then* $\hat{\bar{\lambda}} = -\bar{\xi}_k - i\bar{\eta}_k$ *is also the eigenvalue and the corresponding parameters in* $\bar{v}_{k_0} = [\bar{a}_k, \bar{b}_k]^T$ *and* $\hat{\bar{v}}_{k_0} = [\hat{\bar{a}}_k, \hat{\bar{b}}_k]^T$ *satisfy* $\hat{\bar{a}}_k = \bar{b}_k^*,\ \hat{\bar{b}}_k = \bar{a}_k^*$.

(2). *If* $\xi_k = 0$, *then* $\hat{\bar{\lambda}} = \bar{\lambda} = -i\bar{\eta}_k$, *the corresponding eigenvectors are* $\bar{v}_{k_0} = [1, e^{i\bar{\theta}_k}]$.

*Proof* When the potential matrix satisfies the reduction condition (5), the potential matrix $Q_0$ becomes

$$Q_0 = \begin{bmatrix} 0 & q^*(-x,0) \\ q(x,0) & 0 \end{bmatrix}. \tag{43}$$

It is easy to get that the $Q_0$ above meets the following symmetry relationship

$$Q_0^*(-x) = \sigma Q_0 \sigma, \tag{44}$$

where

$$\sigma = \begin{bmatrix} 0 & 1 \\ 1 & 0 \end{bmatrix}$$

is the Pauli spin matrix. For the scattering equation (13), replacing $x$ by $-x$,

$$J(-x)_x = -i\lambda \Sigma J(-x) + i\lambda J(-x)\Sigma + iQ_0(-x)J(-x) \tag{45}$$

and taking conjugate matrix on both sides of the equation, then we can get that

$$J^*(-x)_x = i\lambda^*\Sigma J^*(-x) - i\lambda^* J^*(-x)\Sigma - iQ_0^*(-x)J^*(-x). \tag{46}$$

Multiplying the Pauli matrix $\sigma$ from left and right to the both sides of the equation, then by the symmetry relation (44), we have the following equation

$$[\sigma J^*(-x)\sigma]_x = i\lambda^*\sigma\Sigma J^*(-x)\sigma - i\lambda^*\sigma J^*(-x)\Sigma\sigma - iQ_0\sigma J^*(-x)\sigma, \tag{47}$$

and by $\sigma\Sigma = -\Sigma\sigma$, we have

$$[\sigma J^*(-x)\sigma]_x = -i\lambda^*[\Sigma, \sigma J^*(-x)\sigma] - iQ_0 \sigma J^*(-x)\sigma. \tag{48}$$

Thus, $\hat{\lambda} = -\lambda^*$ and $\hat{J} = \sigma J^*(-x)\sigma$ also satisfy equation (13). We can infer that $\hat{J}$ and $J$ have the same boundary condition at $x \to \infty$, so they are the same solution of equation (13), i.e., we can get that

$$\hat{J}_k = \sigma J_k^*(-x)\sigma,\ k = 1, 2. \tag{49}$$

By the definition (21), (27) and the symmetry relation (49), we have

$$\hat{P}^{\pm} = \sigma P^{\pm *}(-x)\sigma. \tag{50}$$

Taking the reverse-space transformation and implement conjugation of equation (35),

$$P^{+*}(-x)v_k^*(-x) = 0. \tag{51}$$

and then multiplying $\sigma$ and by (50), we have

$$\sigma P^{+*}(-x)v_k^*(-x) = \sigma P^{+*}(-x)\sigma\sigma v_k^*(-x) = \hat{P}^+\sigma v_k^*(-x) = 0. \tag{52}$$

The solution of the equation $\hat{P}^+\hat{v}_k = 0$ is $\hat{v}_k = \sigma v_k^*(-x)$. So, by the

$$\hat{v}_k = \sigma v_k^*(-x) = \begin{bmatrix} 0 & 1 \\ 1 & 0 \end{bmatrix}\begin{bmatrix} a_k^* e^{-i\theta_k^*} \\ b_k^* e^{i\theta_k^*} \end{bmatrix} = \begin{bmatrix} b_k^* e^{i\theta_k^*} \\ a_k^* e^{-i\theta_k^*} \end{bmatrix} = \begin{bmatrix} \hat{a}_k e^{i\theta_k} \\ \hat{b}_k e^{-i\theta_k} \end{bmatrix}, \tag{53}$$

so $\hat{a}_k = b_k^*,\ \hat{b}_k = a_k^*$.

Implementing the similar process on the adjoint scattering problem (24), then the second rule of Theorem 2 can be proved. The process is easy to get according to the proof above; we omit it here. □

However, for the reverse-time GNLS equation (3) and reverse-space-time GNLS equation (4), the symmetry relations are quite different. □

**Theorem 3** *For the reverse-time NGNLS equation (3), if* $\lambda = \lambda_k$ *is the eigenvalue of the scattering equation (13), then* $\bar{\lambda} = -\lambda_k$ *is the eigenvalue of the adjoint scattering problem (24) and the corresponding parameters in* $v_{k_0} = [a_k, b_k]$ *and* $\bar{v}_{k_0} = [\bar{a}_k, \bar{b}_k]^T$ *satisfy* $\bar{a}_k = a_k,\ \bar{b}_k = b_k$.

*Proof* With the reduction condition (6), the potential matrix $Q_0$ becomes

$$Q_0 = \begin{bmatrix} 0 & -q(x,0) \\ q(x,0) & 0 \end{bmatrix}, \tag{54}$$

so $Q_0$ satisfies the following symmetry relation

$$Q_0 = -Q_0^T. \tag{55}$$

Taking transpose on both sides of the scattering equation (13) and substituting the relation (55), then we have

$$\begin{aligned} J_x^T &= i\lambda J^T\Sigma - i\lambda\Sigma J^T - iJ^T Q_0^T \\ &= -i\lambda[\Sigma, J^T] + iJ^T Q_0, \end{aligned} \tag{56}$$

so $\bar{\lambda} = -\lambda$, $\bar{K} = J^T$ is a solution of the adjoint scattering equation (24). Since $J^{-1}$ also satisfies equation (24). Therefore, $J^T$ and $J^{-1}$ are linearly dependent on each other. Similarly, combining the boundary conditions at $x \to \infty$, we get

$$J_k^{-1} = J_k^T, \; k = 1, 2. \tag{57}$$

By (21), (27) and the symmetry relation (49), we have

$$\bar{P}^- = P^{+T}. \tag{58}$$

Taking the reverse-space transformation and implementing the transpose of the equation (36) and by (66),

$$\bar{P}^{-T}\bar{v}_j^T = P^+\bar{v}_j^T = 0. \tag{59}$$

so by $P^+v_j = 0$, $\bar{v}_j = v_j^T$ and then combined with (42), we have

$$\begin{aligned} \bar{v}_j &= v_j^T = \left(e^{i\theta_k\Sigma}v_{k0}\right)^T = \left[a_k e^{i\theta_k}, b_k e^{-i\theta_k}\right] \\ &= \bar{v}_{j0}e^{-i\bar{\theta}_j\Sigma} = \left[\bar{a}_k e^{i\theta_k}, \bar{b}_k e^{-i\theta_k}\right]. \end{aligned} \tag{60}$$

so we have $\bar{a}_k = a_k, \; \bar{b}_k = b_k$. □

**Theorem 4** *For the reverse-space-time NGNLS equation (4), there are not any restrictions and relationships between the eigenvalues in $\mathbb{C}_+$ and $\mathbb{C}_-$, but the eigenvalues $v_{k0} = [1, \omega_k]$ and $\bar{v}_{k0} = [1, \bar{\omega}_k]$ where $\omega_k = \pm 1, \; \bar{\omega}_k = \pm 1$.*

*Proof* For equation (4), the potential matrix $Q_0$ is

$$Q_0 = \begin{bmatrix} 0 & -q(-x, 0) \\ q(x, 0) & 0 \end{bmatrix}, \tag{61}$$

so we have

$$Q_0(-x) = -\sigma Q_0\sigma. \tag{62}$$

Replacing $x$ by $-x$ in the scattering equation (13), then we obtain

$$[J(-x)]_x = -i\lambda\Sigma J(-x) + i\lambda J(-x)\Sigma + iQ_0(-x)J(-x), \tag{63}$$

and multiplying $\sigma$ on both sides of equation (64) and substituting the relation (62), then we have

$$\begin{aligned} [\sigma J(-x)\sigma]_x &= -i\lambda\sigma\Sigma J(-x)\sigma + i\lambda\sigma J(-x)\Sigma \\ &\quad \sigma + i\sigma Q_0(-x)\sigma\sigma J(-x)\sigma \\ &= -i\lambda\sigma\Sigma J(-x)\sigma + i\lambda\sigma J(-x)\Sigma \\ &\quad \sigma - iQ_0\sigma J(-x)\sigma \\ &= i\lambda[\Sigma, \sigma J(-x)\sigma] - iQ_0\sigma J(-x)\sigma. \end{aligned} \tag{64}$$

So, $\sigma J(-x)\sigma$ is also a solution of the scattering equation (13); combining the boundary conditions at $x \to \infty$, we get

$$\hat{J}_k = \sigma J(-x)\sigma, \; k = 1, 2. \tag{65}$$

By (21), (27) and the symmetry relation (49), we have

$$\hat{P}^+(-x) = P^+(x)\sigma. \tag{66}$$

Take $x$ by $-x$ in (35) and by (66),

$$\hat{P}^+(-x)\hat{v}_j(-x) = P^+\sigma\hat{v}_j(-x) = 0, \tag{67}$$

so by $P^+v_j = 0$, we have $\hat{v}_j(-x) = \omega_j\sigma v_j$ with $\omega_j$ is arbitrary constant, and then combined with (42), we have

$$a_k = \omega_k b_k, \; b_k = \omega_k a_k \tag{68}$$

so we have $\omega_k = \pm 1$. Taking $a_k = 1$, then the corresponding vector is $v_{k0} = [1, \omega_k]^T$. Implementing the similar process, we can get that the corresponding vector is $\bar{v}_{k0} = [1, \bar{\omega}_k]$. □

## 4 Dynamics behaviors of NGNLS equations

The symmetry relations of scattering data in Theorem 2, 3 and 4 determine the structures of soliton solutions for different NGNLS equations (2), (3) and (4). In order to investigate the difference between them, in this section, we exhibit different dynamic behaviors of the one-soliton and two-soliton solutions for the three NGNLS equations.

### 4.1 Dynamics behaviors of reverse-space GNLS equation (2)

Firstly, we consider the reverse-space GNLS equation (2). For $\lambda_k \in \mathbb{C}_+$ and $\bar{\lambda}_k \in \mathbb{C}_-$, by Theorem 2, we consider the following one-soliton and two-soliton solutions.

#### *4.1.1 One-soliton solution for equation (2)*

When $N = 1$ in (37), we can get the expression of one-soliton solution. By Theorem 2, without loss of

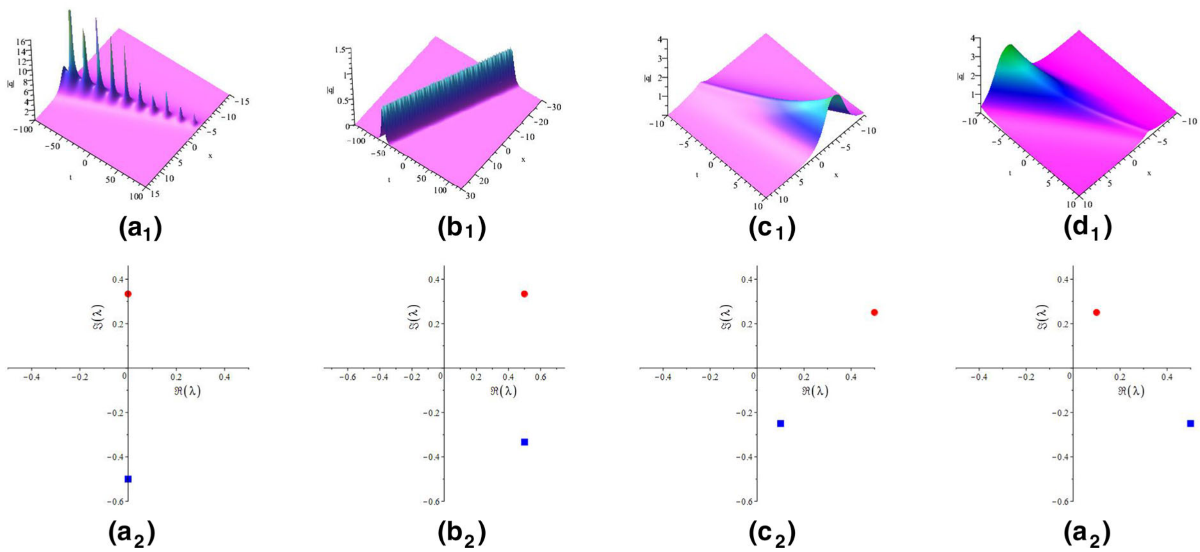

**Fig. 1** One-soliton solutions of the reverse-space GNLS equation (2) and the corresponding configuration of the eigenvalues with parameters $C = [10^{-2}, 5 \times 10^{-2}, 5 \times 10^{-2}]$

generality, taking $a_1 = \bar{a}_1 = 1,\ b_1 = e^{i\rho_1},\ \bar{b}_1 = e^{i\bar{\rho}_1}$, then the one-soliton solution of equation (2) can be obtained

$$q = 2\left(\bar{\lambda}_1 - \lambda_1\right) \mathrm{e}^{\bar{\theta}_1 - \theta_1 + \frac{i}{2}(\rho_1 - \bar{\rho}_1)} \\ sech\left(-\bar{\theta}_1 - \theta_1 + \frac{i}{2}(\rho_1 + \bar{\rho}_1)\right), \tag{69}$$

where $\theta$ and $\bar{\theta}_1$ contains two spectral parameters $\lambda_1 \in \mathbb{C}_+$, $\bar{\lambda}_1 \in \mathbb{C}_-$ and $\rho_1$ and $\bar{\rho}_1$ are any real constants.

By equation (69), when $\theta_1 + \bar{\theta}_1 = \frac{i}{2}(\rho_1 + \bar{\rho}_1 - \pi)$, the solution (69) is singular, and when $\theta_1 + \bar{\theta}_1 \neq \frac{i}{2}(\rho_1 + \bar{\rho}_1 - \pi)$, the one-soliton solution is nonsingular. Under this case, the spectral parameters $\lambda_1 \in \mathbb{C}_+$ and $\bar{\lambda}_1 \in \mathbb{C}_-$ can be arranged as the following three configurations.

Case 1 $\Re(\lambda_1) = \Re(\bar{\lambda}_1) = 0$ and $\Im(\lambda_1) \neq \Im(\bar{\lambda}_1)$. In this case, the single soliton behaves as a breathing soliton collapses to a peak periodically. Figure 1-($a_1$) and ($a_2$) shows the map and the corresponding spectral configuration. For convenience, in Fig.1 the other parameters are taken as

$$\rho_1 = \frac{\pi}{4},\ \bar{\rho}_1 = 0,\ C = [10^{-2}, 5 \times 10^{-2}, 5 \times 10^{-2}]. \tag{70}$$

For $\theta_1$ and $\bar{\theta}_1$ are fifth-order quintic polynomials of $\lambda_1$ and $\bar{\lambda}_1$, we will investigate the influence of the coefficients of high-order terms. When the coefficients of odd powers for the function $f(\lambda)$ are greater than 0, the amplitude increases along the direction of wave propagation. And conversely, when this coefficient is less than 0, the amplitude decreases. Here, we take $C$ as different values to illustrate. When $C = [0.05, 0, 0]$, the height of the breathing soliton gradually increases to infinity from $t = +\infty$ to $t = -\infty$ which is shown in Fig.2-($a$), and when $C = [0, 0, -0.05]$ in Fig.2-($c$), the amplitude of the breathing soliton behaves as the opposite trend. Besides, the trajectory also deflects when coefficients of odd orders for the function $f(\lambda)$ change. However, if $C$ takes $[0, 0.05, 0]$ in Fig.2-($b$), the elements of breathing-soliton are all in same heights and do not increase as time $t$ changes and the trajectory stays parallel to the time axis no matter how $\beta$ changes.

Case 2 If $\lambda_1 = \bar{\lambda}_1^*$.
Under this case, for any $(x, t) \in R^2$, $\theta_1 + \bar{\theta}_1 - \frac{i}{2}(\rho_1 + \bar{\rho}_1)$ is real and this formula cannot be equal to $-\frac{i\pi}{2}$, so the solution is nonsingular for any $(x, t) \in R^2$. Under this case, the solution $|q|$ is a constant-amplitude soliton; this is not different with the local case. The propagation trajectory of the soli-

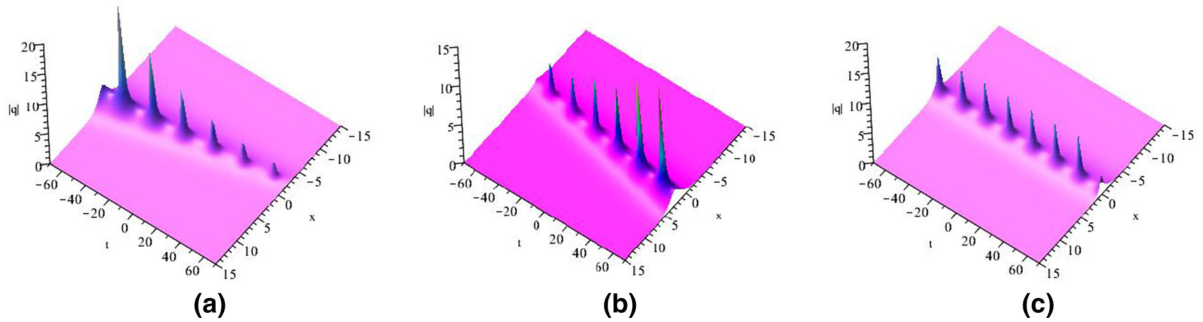


**Fig. 2** One-soliton solution of the reverse-space GNLS equation (2) with different $C$

ton is $\frac{t(207\alpha-61\delta+180\gamma_1-81)}{81}=x$, so when $C$ changes, the soliton will deflect some angles but never parallel to the $x$ axis. We take $\lambda_1=\bar{\lambda}_1^*=\frac{1}{2}+\frac{i}{3}$ to illustrate in Fig.1-($b_1$) and ($b_2$).

Case 3 If $\Im(\lambda_1)=-\Im(\bar{\lambda}_1)$ and $\Re(\lambda_1)\neq\Re(\bar{\lambda}_1)$. In this case, the soliton did not collapse but propagate forward with a varying amplitude which is due to $\Re(\lambda_1)\neq\Re(\bar{\lambda}_1)$. And when $\Re(\lambda_1)>\Re(\bar{\lambda}_1)$, the amplitude grows along the propagation direction, and the figure and the spectral configuration are shown in Fig.1-($c_1$) and ($c_2$) where $\Re(\lambda_1)=\frac{1}{2}$ and $\Re(\bar{\lambda}_1)=\frac{1}{10}$. When $\Re(\lambda_1)<\Re(\bar{\lambda}_1)$, the amplitude drops along the propagation direction, and the figure and the spectral configuration are shown in Fig.1-($d_1$) and ($d_2$) where $\Re(\lambda_1)=\frac{1}{10}$ and $\Re(\bar{\lambda}_1)=\frac{1}{2}$.

### *4.1.2 Two-soliton solutions for equation (2)*

Next, we consider the dynamic behaviors of two-soliton solutions. Taking $N=2$ in the solution (37)and by Theorem 2, the two-soliton solutions for equation (2) can be obtained. The expression of the two-soliton solution is tremendous; we omit it here. In this case, together with the free parameters $C$ in the function $f$, there are still 15 free parameters in total in this two-soliton solution $\lambda_k, \bar{\lambda}_k, a_k, \bar{a}_k, b_k, \bar{b}_k, k=1,2$ and $C$. By Theorem 2, $\lambda_k\in\mathbb{C}_+$ and $\bar{\lambda}_k\in\mathbb{C}_-$, $k=1,2$ are four eigenvalues which can be irrelevant to each other. Combining the symmetry relations of eigenvalues for the reverse-space system in Theorem 2, the values of the four independent eigenvalues can be listed as the following configurations.

Case 1 If $\Re(\lambda_k)=\Re(\bar{\lambda}_k)=0, k=1,2$. In this case, the spectral parameters $\lambda_k, \bar{\lambda}_k$ are all pure imaginary numbers. Without loss of generality, we take $a_k=\bar{a}_k=1$, $b_k=e^{i\rho_k}$, $\bar{b}_k=e^{i\bar{\rho}_k}$, $(k=1,2)$; then the two-soliton solution contains four real parameters $\rho_k, \bar{\rho}_k (k=1,2)$ and four complex eigenvalues. When $\Im(\lambda_k)=\Im(\bar{\lambda}_k)$ $(k=1,2)$, the two-soliton solution behaves as a new soliton collapse periodically. But with different choices of the spectral parameter, this new type of two-soliton solution behaves different nonlinearity. The plots of this new two-soliton solution are shown in Fig.3-($a_1$) and ($a_2$) where the parameters are taken as

$$
\begin{aligned}
&\lambda_1=\frac{3i}{5},\ \bar{\lambda}_1=-\frac{i}{5},\\
&\lambda_2=\frac{2i}{3},\ \bar{\lambda}_2=-\frac{i}{3},\\
&\rho_1=\frac{\pi}{4},\ \bar{\rho}_1=\rho_2=0,\ \bar{\rho}_2=\frac{\pi}{3},\\
&C=[10^{-2},5\times10^{-2},5\times10^{-2}].
\end{aligned}\tag{71}
$$

We can see that the two-soliton solution exhibits periodic singularities, but the two solitons included are entangled and with different heights on both sides. Besides, different from the case in [23] where the soliton does not move, the trajectory of the solution is deflected over time and is no longer parallel to the $t$-axis. However, when we take the cubic and quintic terms zero, i.e., take $C=[0,5\times10^{-2},0]$, the wave will not move as time changes which is similar to the case in [23]. The deflection is due to the cubic and quintic terms.

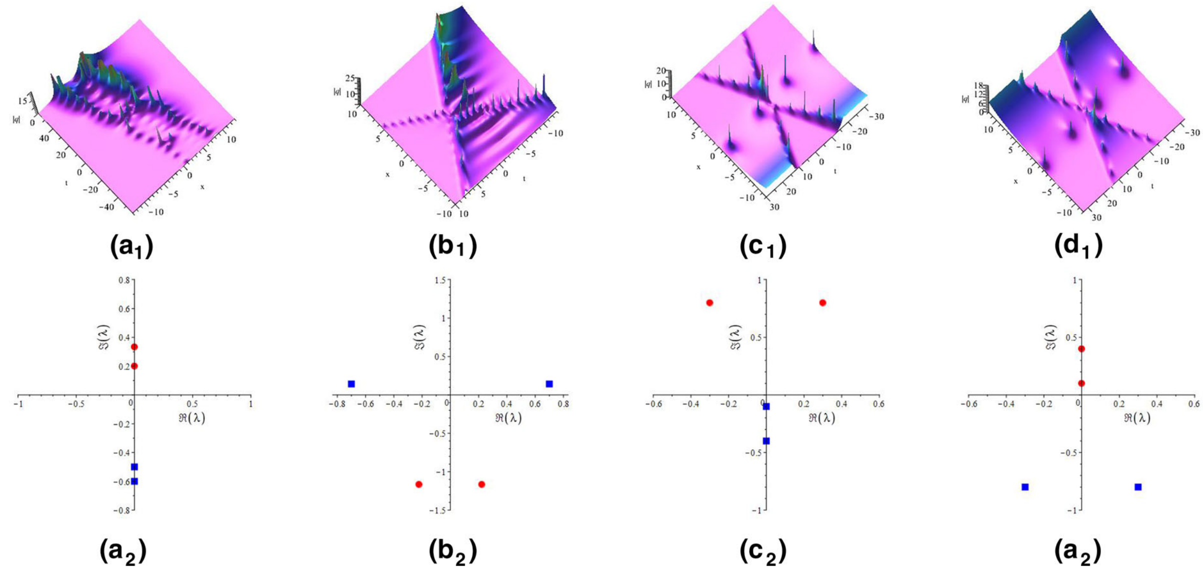


**Fig. 3** Two-soliton solutions of the reverse-space equation (2) and the corresponding configuration of the eigenvalues with $C = [10^{-2}, 5\times 10^{-2}, 5\times 10^{-2}]$

Case 2 $\lambda_k \in \mathbb{C}_+$, $\bar{\lambda}_k \in \mathbb{C}_-$ and $\lambda_2 = -\lambda_1^*$, $\bar{\lambda}_2 = -\bar{\lambda}_1^*$.

In this case, the solution $|q|$ is a periodically singular two-solitary wave. It consists of two crossed singular solitary waves. And the amplitude of singular solitary waves changes exponentially with time. Here, we take the parameters

$$\begin{aligned}&\lambda_1 = -\lambda_2{}^* = \frac{7}{10} + \frac{i}{7},\\ &\bar{\lambda}_1 = -\bar{\lambda}_2^* = \frac{2}{9} - \frac{7i}{6},\\ &a_1 = \bar{a}_1 = b_2 = \bar{b}_2 = 1,\ a_2 = b_1^* = 2 - i,\\ &\bar{a}_2 = \bar{b}_1^* = -\frac{i}{5},\end{aligned} \tag{72}$$

to explain. The corresponding figure and the spectral configuration are shown in Fig.3-$(b_1)$ and $(b_2)$. We can see that the amplitudes of the two solitons both increase exponentially with time. The directions of the movement of two singular solitons are also different. But the solution is not a simple nonlinear superposition of two singular solitons.

Case 3 If $\lambda_1 = -\lambda_2^* \neq 0$ and $\Re(\bar{\lambda}_k) = 0$ $(k = 1, 2)$. By Theorem 1, when $\lambda_2 = -\lambda_1^*$, the eigenvectors $a_2 = b_1^*$ and $b_2 = a_1^*$. In this case, the solution behaves as a new two-soliton waves which consisted of three waves that collapse repeatedly. We take

$$\begin{aligned}&\lambda_1 = -\lambda_2{}^* = \frac{3}{10} + \frac{4}{5}i,\ \bar{\lambda}_1 = -\frac{2}{5}i,\\ &\bar{\lambda}_2 = -\frac{i}{10},\\ &a_1 = \bar{a}_1 = b_2 = -\bar{b}_2 = \bar{a}_2 = 1,\\ &a_2 = b_1^* = 1 - i,\ \bar{b}_1 = \frac{\sqrt{2}}{2}(1 - i).\end{aligned} \tag{73}$$

to declare. The spectral configuration and the corresponding figure are shown in Fig.3-$(c_1)$ and $(c_2)$. We can see that there is a singular wave near $x = 0$ and two traveling waves crossed with the standing wave. It is mentioned that the amplitude of the middle wave did not change, but the amplitudes of the other two traveling waves increase exponentially and decrease exponentially, respectively. Different from the classical NLS equation [23], the singular wave in the middle deflects some angle under the influence of the high-order terms.

Case 4 If $\Re(\lambda_k) = 0 (k = 1, 2)$ and $\bar{\lambda}_1 = -\bar{\lambda}_2^* \neq 0$. The spectral configuration and the corresponding figure are shown in Fig.3-$(d_1)$ and $(d_2)$, where the spectral parameters are

$$\bar{\lambda}_1 = -\bar{\lambda}_2^* = \tfrac{3}{10} - \tfrac{4}{5}i,\ \lambda_1 = \tfrac{2}{5}i,\ \lambda_2 = \tfrac{i}{10} \tag{74}$$

We can see that the changing trend of amplitudes is opposite with other parameters being same as Case 3. The two-soliton solution is similar to the solution of Case 3.

#### 4.1.3 Bound state two-soliton solutions for equation (2)

In fact, for Case 2, when $\lambda_1 = \bar{\lambda}_1^*$, $\lambda_2 = \bar{\lambda}_2^*$ or $\lambda_1 = \bar{\lambda}_2^*$, $\lambda_2 = \bar{\lambda}_1^*$, the two-soliton solution is nonsingular and remains bounded with time. Due to the diversity of parameter values, we exhibit the case $\lambda_1 = \bar{\lambda}_1^*$, $\lambda_2 = \bar{\lambda}_2^*$. With different values of $C$, the bound state is quite different with the case in [23]. It is interesting that when the coefficients of the cubic or quintic terms are not 0, the bounded soliton degenerates to the ordinary two soliton, but the situation is completely different from the ordinary two solitons when two solitons collide. When $C = [10^{-2}, 5\times10^{-2}, 5\times10^{-2}]$, the corresponding figure is shown in Fig. 4-$(a_1)$, and the magnification detailed plots of the intersection are shown in Fig. 4-$(a_2)$, the peaks in the middle are deflected as time changes which differ from the bound state for the reverse-space NLS equation [23]. However, when the coefficients of the cubic and quintic terms are 0 in Fig. 4-$(b_1)$ and $(b_2)$, the bounded soliton is similar to the corresponding case in [23]. Without loss of generality, the other parameters in Fig. 4-$(a)$ and $(b)$ are

$$\rho_1 = -\bar{\rho}_1 = -\frac{\pi}{3},\ \rho_2 = \bar{\rho}_2 = 0,$$
$$\lambda_1 = -\bar{\lambda}_1 = \frac{i}{5},$$
$$\lambda_2 = -\bar{\lambda}_2 = \frac{i}{3}. \tag{75}$$

For Case 3, if $\Im(\lambda_1) = -\Im(\bar{\lambda}_1)$ and $\Re(\lambda_1) \neq \Re(\bar{\lambda}_1)$, when $C = [10^{-2}, 5\times10^{-2}, 5\times10^{-2}]$, we can get the nonsingular solution as shown in Fig. 4-$(c_1)$, where the two-solitary wave stay bounded at the beginning, but as $t \to \pm\infty$, the amplitudes tend to infinity with different directions. Besides, when two solitons collide, the intersection is breathing but is not symmetric about the zero point with the changing amplitudes. The enlarged view of collision is shown in Fig. 4-$(c_2)$. The increase of the amplitudes is due to the difference of the real part $\Re(\lambda_1) \neq \Re(\bar{\lambda}_1)$. The parameters of Fig. 4-$(c_1)$ and $(c_2)$ are

$$\lambda_1 = -\lambda_2^* = \frac{7}{10} + \frac{i}{4},\ \bar{\lambda}_1 = -\bar{\lambda}_2^* = \frac{9}{10} - \frac{i}{4},$$
$$[a_1, b_1] = -\left[\bar{a}_1, \bar{b}_1\right] = [1, 1+i]$$
$$,\left[\bar{a}_2, \bar{b}_2\right]$$
$$= [a_2, b_2] = [-1, -1]. \tag{76}$$

Besides, when $\Re(\lambda_1) = \Re(\bar{\lambda}_1)$, the two solitary waves collide elastically and the amplitudes do not change with time. The wave will always be bounded. Taking the same $C$ as in Fig. 4-$(c_1)$, Fig. 4-$(d_1)$ and $(d_2)$ shows the plot and the enlarged view of intersection with parameters

$$\lambda_1 = \bar{\lambda}_1^* = -\lambda_2^* = -\bar{\lambda}_2 = \frac{2}{9} + \frac{i}{7},$$
$$\left[\bar{a}_1, \bar{b}_1\right] = [b_2, a_2] = [-1, -2+i],$$
$$[a_1, b_1] = -\left[\bar{b}_2, \bar{a}_2\right] = [1, 2+i]. \tag{77}$$

### 4.2 Dynamics behaviors of reverse-time equation (3)

By Theorem 3, when $\lambda_k$ is the eigenvalues of the scattering equation (13), $\bar{\lambda}_k = -\lambda_k$ is the eigenvalues of the adjoining scattering equation (24). Without loss of generality, take $a_k = \bar{a}_k = 1$, $k = 1, 2, \ldots, N$, and by the corresponding parameters $b_k = \bar{b}_k$.

#### 4.2.1 One-soliton solutions for equation (3)

When $N = 1$ in (37) and by Theorem 2, $\bar{b}_1 = b_1$ and $\bar{\lambda}_1 = \lambda_1$, take $a_1 = \bar{a}_1 = 1$, then the one-soliton solution of equation (2) can be obtained where $\theta$ and $\bar{\theta}_1$ contain two spectral parameters $\lambda_1 \in \mathbb{C}_+$, $\bar{\lambda}_1 \in \mathbb{C}_-$ and $\rho_1$ and $\bar{\rho}_1$ are any real constants.

$$q = -4\lambda_1 \frac{e^{\bar{\theta}_1 - \theta_1}}{b_1 e^{\bar{\theta}_1+\theta_1} + \left(b_1 e^{\bar{\theta}_1+\theta_1}\right)^{-1}}, \tag{78}$$

By equation (78), when $b_1 e^{\bar{\theta}_1+\theta_1} = i$, the soliton is singular. So if $\Re(\lambda_1) = 0$ and $b_1$ is a real number, the soliton (78) solution has no singularity and behaves as a fundamental soliton. Next, we study the situation when $\Re(\lambda_1) \neq 0$. We mainly consider the influence of the fifth-order term of the reverse-time GNLS equation (3), so we only consider the situation when $\beta \neq 0$ and other parameters are zeros. Other situations can also be studied in a similar way.

When the absolute value of $\beta$ is small, the soliton solution behaves as a amplitude-varying wave and it does not collapse and move as time go on. However, with the value of $\beta$ growing, wave packets start to appear where the amplitude of the soliton is small.

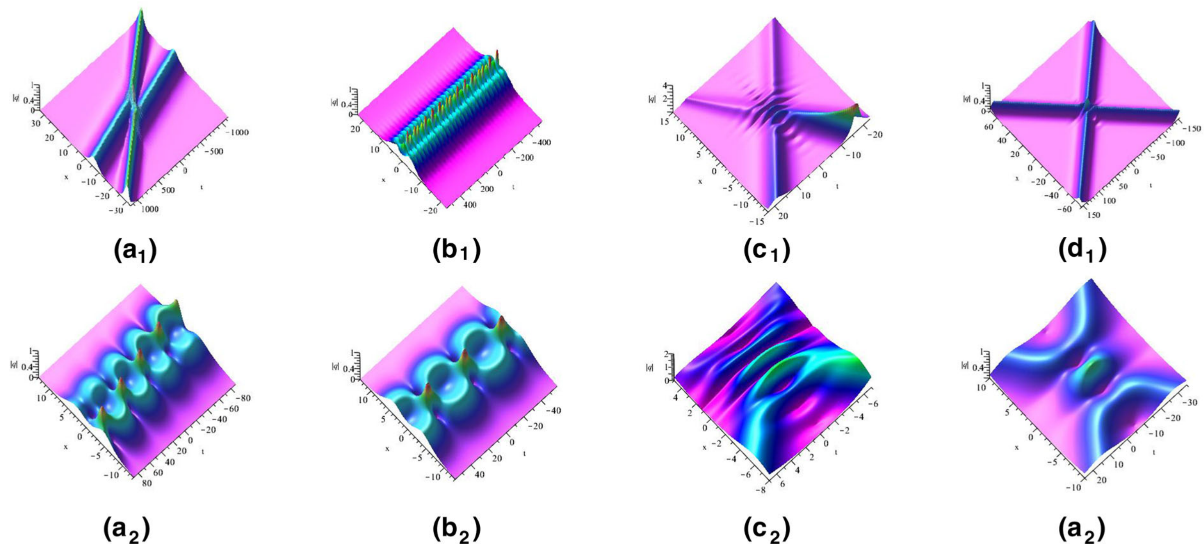


**Fig. 4** Bound states of two-soliton solutions of the reverse-space equation (2) and the corresponding magnification detail plots

As the value of $\beta$ increases, more wave packets begin to appear and a soliton that periodically collapses is formed. This phenomenon is absent in classical equations in [23]. Besides, the trajectory of the wave also begins to deflect as the value of $\beta$ increases.

The amplitude of the soliton increases or decreases with time which is depended by the sign of $\Re(\lambda_1)$. When $\Re(\lambda_1) > 0$, the amplitude grows with time, and when $\Re(\lambda_1) < 0$, the amplitude decays with time. In Fig. 5-($a$) and ($c$) with $\Re(\lambda_1) = 10^{-1}$, their heights are increasing along the propagation direction, and in Fig. 5-($b$) and ($d$) with $\Re(\lambda_1) = -10^{-1}$, the amplitude shows the opposite trend. Fig. 5-($a$) and ($b$) shows the amplitude increasing and decreasing solitons where the parameter $\beta = 5 \times 10^{-1}$. When the coefficient of the fifth-order term $\beta$ grows to 1, we can get the periodic collapsed solitons with varying amplitude which are shown in Fig. 5-($c$) and ($d$). The other parameters in Fig. 5 are same with $\Im(\lambda_1) = \frac{1}{2}$ and $b_1 = 1 + \frac{i}{2}$.

By the analysis above, we can see that the nonlocal fifth-order terms play an important role in the evolutionary behavior of soliton; compared to the classical reverse-time NLS equation in [23], the nonlocal reverse-time GNLS equations has a richer dynamic behavior for the solitons.

#### *4.2.2 Two-soliton solutions for equation* (3)

When we take $N = 2$ in the $N$-soliton solutions, we can get the two-soliton solutions for the (3). By Theorem 3, we can get that $\bar{\lambda}_k = -\lambda_k$ and for the sake of convenience, set $a_k = \bar{a}_k = 1$, $b_k = \bar{b}_k$ $(k = 1, 2)$. Through our analysis, in this case, the higher-order term coefficients do not affect the basic classification of eigenvalues configurations. So, we consider the following eigenvalues configurations.

Firstly, when $\Im(\lambda_1) \neq \Im(\lambda_2)$, $\Re(\lambda_1) \neq \Re(\lambda_2)$ and $\Im(\lambda_k)\Re(\lambda_k) \neq 0, k = 1, 2$. With various values of $b_k(k = 1, 2)$, the two-soliton solution is singular wave consisted by two amplitude-changing singular solitary wave. Fig. 6-($a_1$) and ($a_2$) shows the corresponding plot and configuration, where the parameters are

$$\lambda_1 = -\bar{\lambda}_1 = \frac{1}{10} + \frac{i}{4}, \lambda_2 = -\bar{\lambda}_2 = \frac{1}{20} - \frac{i}{2}, b_1 = 1 + \frac{i}{2},\ b_2 = -i. \tag{79}$$

Secondly, when $\Im(\lambda_1) = \Im(\lambda_2)$, $\Re(\lambda_1) \neq \Re(\lambda_2)$ and $\Im(\lambda_k)\Re(\lambda_k) \neq 0, k = 1, 2$. In this case, $|q|$ is a nonsingular wave consisted by crossed two amplitude-changing solitary waves. The changing trend is also determined by the difference between $|\Re(\lambda_k)|(k = 1, 2)$. And when $|\Re(\lambda_1)| > |\Re(\lambda_2)|$, the amplitude grows with time; we take

$$\lambda_1 = -\bar{\lambda}_1 = \frac{1}{5} + \frac{i}{10}, \lambda_2 = -\bar{\lambda}_2 = -\frac{1}{8} + \frac{i}{10}, b_1 = \frac{i}{2}, b_2 = \frac{1}{3}, \tag{80}$$

to illustrate, the figure and the corresponding spectral configuration are shown in Fig. 6-($b_1$) and ($b_2$).

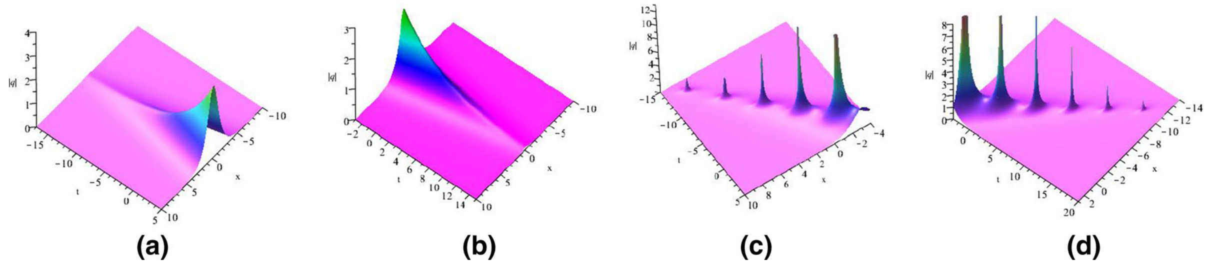

**Fig. 5** One-soliton solutions of the reverse-time equation (2)

Besides, when $|\Re(\lambda_1)| < |\Re(\lambda_2)|$, the amplitude of two waves decreases with time. Changing the value of $\lambda_2$ only in 80 and taking $\lambda_2 = -1/4 + \frac{i}{10}$, we can get the decreasing wave and the spectral configuration in Fig. 6-($c_1$) and ($c_2$).

Thirdly, if $\lambda_1 = -\lambda_2^*$ and the eigenvectors $\upsilon_{10} = \upsilon_{20}^*$, the amplitude of two waves will not change with time, the plot and the corresponding spectral configuration with

$$\lambda_1 = -\bar{\lambda}_1 = \frac{1}{10} + \frac{i}{3},\ \lambda_2 = -\bar{\lambda}_2 = -\frac{1}{10} + \frac{i}{3},\ b_1 = b_2^* = 1 + \frac{i}{2}. \tag{81}$$

which are exhibited in Fig. 6-($d_1$) and ($d_2$).

### 4.3 Dynamics behaviors of reverse-space-time equation (4)

By Theorem 4, when $N$=1, we can get the one-soliton solution for the reverse-time equation (4)

$$|q| = \frac{-2\omega_1\left(-\bar{\lambda}_1 + \lambda_1\right) \mathrm{e}^{-2i\lambda_1\left(16\beta\lambda_1{}^4+\lambda_1\right)t-2i\lambda_1 x}}{1 + \omega_1\omega_1 \mathrm{e}^{-2i\left(16\beta\lambda_1{}^5-16\beta\bar{\lambda}_1^5+\lambda_1{}^2-\bar{\lambda}_1^2\right)t-2i\left(-\bar{\lambda}_1+\lambda_1\right)x}}, \tag{82}$$

where $\omega_1$ and $\bar{\omega}_1$ can be $\pm 1$. The velocity is

$$\upsilon = -\frac{16\beta\Im(\lambda_1{}^5 - \bar{\lambda}_1^5) + \Im(\lambda_1{}^2 - \bar{\lambda}_1^2)}{\Im\left(\lambda_1 - \bar{\lambda}_1\right)}.$$

The amplitude of $|q|$ changes when $x = \upsilon t$, and the expression can be exhibited as

$$|q(t)| = 2|\lambda_1 - \bar{\lambda}_1| \frac{e^{At}}{1 + \omega_1\bar{\omega}_1 e^{iBt}} \tag{83}$$

where

$$A = 2\Im(\lambda_1)\upsilon + 32\beta\Im(\lambda_1^5) + 2\Im(\lambda_1^2),$$
$$B = -2\Re(\lambda_1 - \bar{\lambda}_1)\upsilon - 32\beta\Re(\lambda_1^5 - \bar{\lambda}_1^5) - 2\Re(\lambda_1^2 - \bar{\lambda}_1^2).$$

Substituting the $\upsilon$ into the above equations, we have

$$A = \frac{-4\Im(\lambda_1)\Im(\bar{\lambda}_1)A_0}{\Im(\lambda_1 - \bar{\lambda}_1)},$$
$$B = \frac{2\left[\Im\left(\lambda_1 - \bar{\lambda}_1\right)^2 + \Re\left(\lambda_1 - \bar{\lambda}_1\right)^2\right]B_0}{\Im(\lambda_1 - \bar{\lambda}_1)}.$$

with

$$\begin{aligned} A_0 = &\Big[8\Im\left(\bar{\lambda}_1\right)^4 - 80\Im\left(\bar{\lambda}_1\right)^2\Re\left(\bar{\lambda}_1\right)^2 + 40\Re\left(\lambda 10\right)^4 - 8\\ &\Im\left(\lambda_1\right)^4 + 80\Im\left(\lambda_1\right)^2\Re\left(\lambda_1\right)^2\\ &-40\Re\left(\lambda_1\right)^4\Big]\beta + \Re\left(\bar{\lambda}_1 - \lambda_1\right),\end{aligned}$$

$$\begin{aligned} B_0 = &\Big[64\Im\left(\bar{\lambda}_1\right)^3\Re\left(\bar{\lambda}_1\right) + 16\Im\left(\bar{\lambda}_1\right)^3\Re\left(\lambda_1\right)\\ &+48\Im\left(\bar{\lambda}_1\right)^2\Re\left(\bar{\lambda}_1\right)\Im\left(\lambda_1\right)\\ &+32\Im\left(\bar{\lambda}_1\right)^2\Im\left(\lambda_1\right)\Re\left(\lambda_1\right) - 64\Im\left(\bar{\lambda}_1\right)\Re\left(\bar{\lambda}_1\right)^3\\ &-48\Im\left(\bar{\lambda}_1\right)\Re\left(\bar{\lambda}_1\right)^2\Re\left(\lambda_1\right)\\ &+32\Im\left(\bar{\lambda}_1\right)\Re\left(\bar{\lambda}_1\right)\Im\left(\lambda_1\right)^2 - 32\Im\left(\bar{\lambda}_1\right)\Re\left(\bar{\lambda}_1\right)\\ &\Re\left(\lambda_1\right)^2 + 48\Im\left(\bar{\lambda}_1\right)\Im\left(\lambda_1\right)^2\Re\left(\lambda_1\right)\\ &-16\Im\left(\lambda 10\right)\Re\left(\lambda_1\right)^3 - 16\Re\left(\bar{\lambda}_1\right)^3\Im\left(\lambda_1\right)\\ &-32\Re\left(\bar{\lambda}_1\right)^2\\ &\Im\left(\lambda_1\right)\Re\left(\lambda_1\right)\\ &+16\Re\left(\bar{\lambda}_1\right)\Im\left(\lambda_1\right)^3 - 48\Re\left(\bar{\lambda}_1\right)\\ &\Im\left(\lambda_1\right)\left(\Re\left(\lambda_1\right)\right)^2 + 64\Im\left(\lambda_1\right)^3\Re\left(\lambda_1\right)\\ &-64\Im\left(\lambda_1\right)\Re\left(\lambda_1\right)^3\Big]\beta - \Im\left(\bar{\lambda}_1 + \lambda_1\right).\end{aligned}$$

If $A \neq 0$, i.e., $A_0 \neq 0$, the amplitude changes exponentially with time, and when $A = 0$, the amplitude will be a constant. Moreover, if $B \neq 0$, this soliton is singular at some time, i.e., it collapses periodically with period $\frac{2\Pi}{B}$. The soliton will not be singular and $\omega\bar{\omega} = 1$ and $B = 0$. Here, we take the following sets of values.

We take the values in Table 1 to illustrate. Among them, the values of set $[m]$ ($m = 1, 2, ...5$) are related to the evolution plots and the eigenvalue configurations of $|q|$ in Fig. (7)-($a$), ($b$)...($d$), respectively. When the real and imaginary parts of the two sets of eigenvalues are not equal, i.e., the eigenvalues and the corresponding eigenvectors $\lambda_1$, $(a_1, b_1)$, $\bar{\lambda}_1$ and $\left(\bar{a}_1, \bar{b}_1\right)$ take the values of group [1] and [2] in Table 1, we can get the periodically collapse one-soliton solution for the reverse-time Eq. (4) when the amplitude is increasing

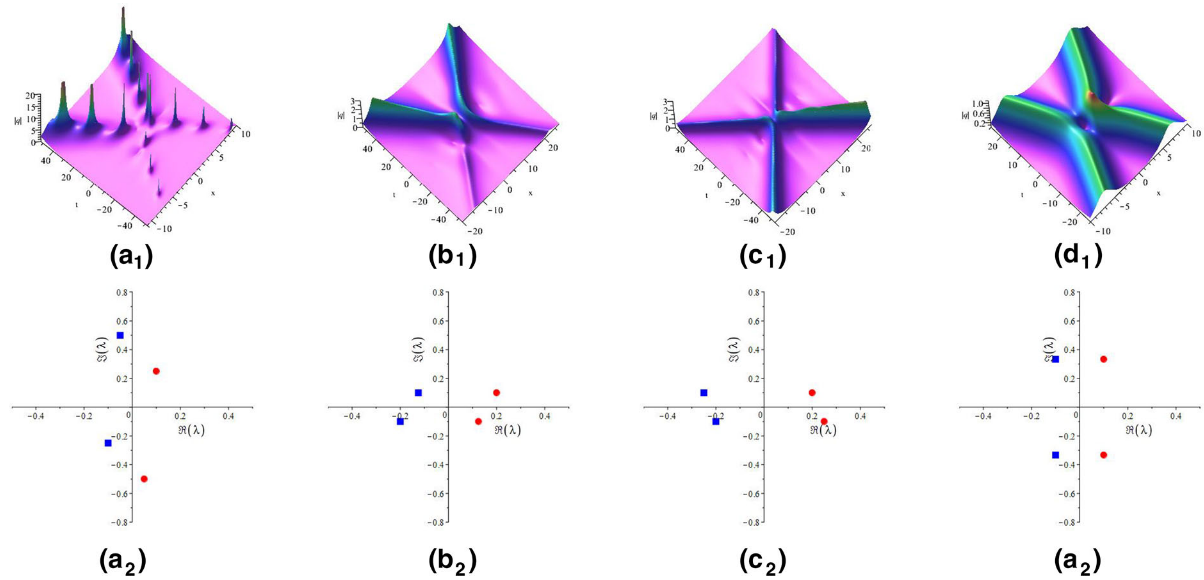


**Fig. 6** Two-soliton solutions and the corresponding spectral configurations of the reverse-time equation (2)

**Table 1** Values under reverse-space-time reduction

| Number | $\lambda_k$ | $(a_k, b_k)$ | $\bar{\lambda}_k$ | $(\bar{a}_k, \bar{b}_k)$ |
|---|---|---|---|---|
| [1] | $-\frac{3}{10}+\frac{9}{10}i$ | $(1, 1)$ | $-\frac{1}{5}-\frac{2}{5}i$ | $(1, -1)$ |
| [2] | $\frac{2}{5}+\frac{i}{10}$ | $(1, 1)$ | $\frac{3}{10}-\frac{3}{5}i$ | $(1, -1)$ |
| [3] | $\frac{2}{9}+\frac{4}{3}i$ | $(1, 1)$ | $\frac{2}{9}-\frac{4}{3}i$ | $(1, 1)$ |
| [4] | $\frac{1}{30}+\frac{2}{3}i$ | $(1, 1)$ | $\frac{1}{10}-\frac{2}{3}i$ | $(1, 1)$ |
| [5] | $\frac{1}{10}+\frac{i}{3}$ | $(1, 1)$ | $-\frac{1}{5}-\frac{i}{4}$ | $(1, 1)$ |

and decreasing, respectively, in Fig. (7)-($a$), ($b$). Figure (7)-($c$) shows the evolution plot the eigenvalue configuration of the fundamental one soliton when $\lambda_1 = \bar{\lambda}_1$. Besides, Fig. (7)-($d$) and ($e$) shows the evolution plots the eigenvalue configurations of the nonsingular one solitons with changing amplitudes.

Next, we consider the nonlinear superposition of one-soliton in Fig. 7. We found that the direct nonlinear superpositions of the values directly lead to the overlay of the evolutionary behaviors. This is a very interesting phenomenon, and the reverse-space and reverse-time equations do not maintain.

According to this phenomenon, we can get some new two two-solitary solutions by the superpositions directly of two set values of single-soliton solutions which is shown in Fig. 8. In order to express conveniently, we sign $[m_1, m_2]$ $(m_1, m_2 = 1, 2..5)$ as $\lambda_1$, $(a_1, b_1)$, $\bar{\lambda}_1$ and $(\bar{a}_1, \bar{b}_1)$ take the values of group $[m_1]$ in table 1 and $\lambda_2$, $(a_2, b_2)$, $\bar{\lambda}_2$ and $(\bar{a}_2, \bar{b}_2)$ take the values of group $[m_2]$ in table 1. When the values are taken as $[1, 2]$, the periodically collapsed two-soliton solution is consisted of two periodically collapsed single solitons. It can be seen from Fig. 8-($a$) that it is completely a nonlinear superposition of the ($a$) and ($b$) of Fig. 7. Besides, we can get the two-soliton solution containing a singular periodically collapsed soliton and a constant-amplitude soliton in Fig. 8-($b$) with the values $[1, 3]$. The two-soliton solution consisted of a periodically collapsed singular soliton and amplitude-decreasing soliton in Fig. 8-($c$) with the values $[1, 4]$ and two-soliton solution consisted of a constant-amplitude soliton and a amplitude-decreasing soliton in Fig. 8-($d$) with the values $[3, 4]$. Furthermore, with changing $\beta$, the fifth-order terms did not influence the property of nonlinear superposition for the reverse-space-time equation (4) via a wide range of parameter values.

## 5 Conclusion

In conclusion, we have constructed the RHP of the GNLS system (1) and exhibited the general new N-soliton solutions for NGNLS (2), (3) and (4). In [28], they only investigated the influences of the highest order terms for the dynamic behaviors of solitons; here,

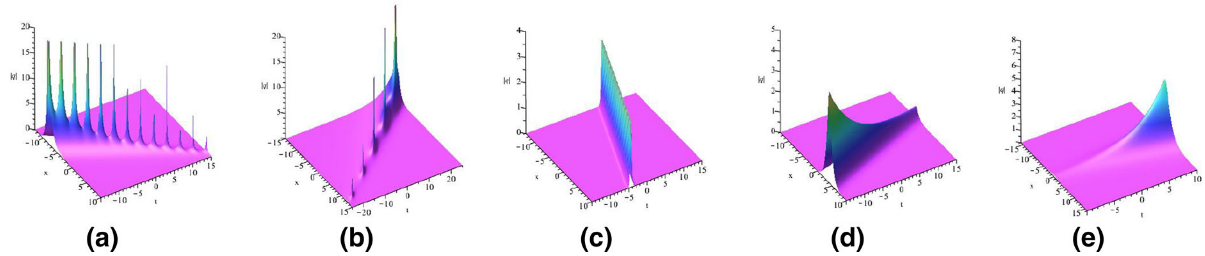


**Fig. 7** One-soliton solutions of the reverse-space-time equation (4)

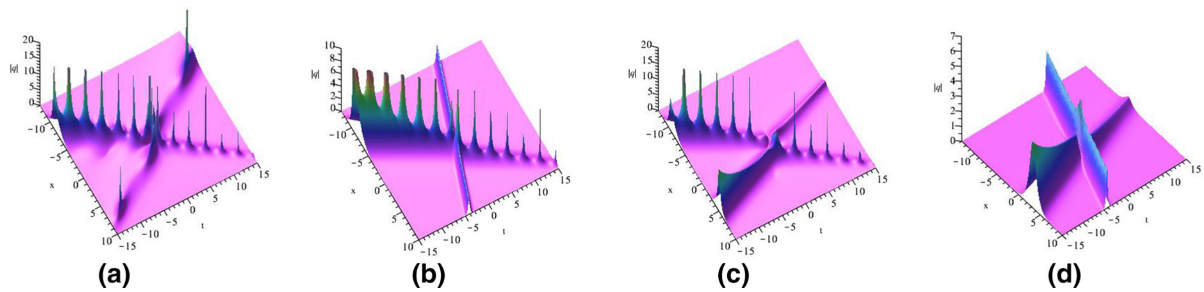


**Fig. 8** Two-soliton solutions of the reverse-space-time equation (4)

we analyzed the third-, fourth- and fifth-order terms and their mixed effects. In [35], by Darboux transformation, some new structures of solutions were obtained, but the distribution of the spectrum to the structures of the solutions could not be analyzed. However, by Riemann–Hilbert problem, we not only found the influence of the distribution of the spectrum and the coefficients of higher-order terms but also obtained some novel features of the dynamic behaviors of the one-soliton and two-soliton solutions for the NGNLS system.

By the various symmetry relations of the scattering data for the reverse-space, reverse-time and reverse-space-time NGNLS Eq. (2), (3) and (4), some novel soliton solutions for the NGNLS equations which are quite different with the local ones are obtained. Besides, there are great differences of the soliton behaviors between the NGNLS equations and the GNLS equation. The dynamic behaviors of the one-soliton and two-soliton solutions have been analyzed for the NGNLS equations.

For the reverse-space NGNLS equation (2), we found some novel features of the dynamic behaviors of the one-soliton and two-soliton solutions. Firstly, as for the singular one-soliton solution, the sign of the coefficients of the cubic and quintic terms $\alpha$ and $\beta$ determines the amplitude-changing trend for singular one-soliton solution. If $\alpha > 0$, the amplitude of the singular one-soliton solution that collapses periodically grows with time. On the contrary, it decreases with time. Besides, new two-soliton solutions under four different spectral configurations for equation (2) were obtained. Some of the two-soliton solutions are similar to the result of the classical nonlocal NLS equation in [23]; however, the solutions of Case 1 and Case 2 are quite different, the higher-order terms bring stronger deformations and deflections of the solutions which lead to the different shapes and transmissions over time. When referring to the bound states of the two-soliton solution, in Fig. 4-($a_1$), when $C \neq 0$, the intersection of two solitons behaves as a breathing waves whose crest is deflected. But when $C = 0$, the solution keeps breathing over time.

For the reverse-time NGNLS equation (3), there is an interesting phenomenon of the one-soliton solution. When the parameter $\beta$ is small, the soliton behaves as a amplitude-changing soliton. As the value of $\beta$ increases, the soliton began to become singular. The changing trend of the soliton is affected by the sign of $\Re(\lambda_1)$. For two-soliton solutions, we get three new kinds of solutions of equation (3) that is quite different with the reverse-space equation (2). The three solutions are shown in Fig.6-($a$), ($b$) and ($c$), respectively.

However, the two-soliton solutions do not describe a nonlinear superposition of fundamental solitons both in NGNLS equations (2) and (3).

For the reverse-space-time NGNLS equation (4), through direct parameter superposition, the corresponding two-soliton solutions were also a direct nonlinear superposition of the two one-soliton waves. By this particular property, we found some new structures of the two-soliton solutions. Three novel two-soliton solutions for the equation (4) that the previous two NGNLS equations (2) (3) did not possess are shown in Fig.8. They are the two-soliton waves composed of a singular single soliton with variable amplitude and a nonsingular single soliton with constant amplitude, the two-soliton waves composed of a singular single soliton with variable amplitude and a nonsingular single soliton with variable amplitude and the two-soliton waves composed of a nonsingular single soliton with variable amplitude and a nonsingular single soliton with constant amplitude, respectively.

These findings reveal the novel and rich soliton structures of the three nonlocal equations (2), (3) and (4) and allow further research of multi-solitons in the other nonlocal equations. It also has some significance for studying other solutions of various nonlocal systems and avoiding some situations in the future.

**Acknowledgements** The authors gratefully acknowledge the support of National Natural Science Foundation of China (No. 11675054), Science and Technology Commission of Shanghai Municipality (No. 18dz2271000) and Future Scientist and Outstanding Scholar Cultivation Program of East China Normal University (No.WLKXJ202001).

**Declarations**

**Conflict of interest** The authors declare that there is no conflict of interests regarding the publication of this paper.

## References

1. Gardner, C.S., Greene, J.M., Kruskal, M.D., Miura, R.M.: Nonlinear-evolution equations of physical significance. Phys. Rev. Lett. **31**(2), 125–127 (1973)
2. Zakharov, V.E., Shabat, A.B.: Exact theory of two-dimensional self-focusing and one-dimensional self-modulation of waves in nonlinear media. J. Exp. Theor. Phys. **34**, 62–69 (1972)
3. Ablowitz, M.J., Kaup, D.J., Newell, A.C., Segur, H.: The inverse scattering transform-Fourier analysis for nonlinear problems. Stud. Appl. Math. **53**(4), 249–315 (1974)
4. Ablowitz, M.J., Clarkson, P.A.: Solitons. Cambridge University Press, Cambridge, Nonlinear evolution equations and inverse scattering (1991)
5. Ablowitz, M.J., Fokas, A.S.: Complex variables, introduction and applications. Cambridge University Press, Cambridge (2003)
6. Novikov, S., Manakov, S. V., Pitaevskii, L. P., Zakharov, V. E.: Theory of Solitons:the Inverse Scattering Method. (1984)
7. Bender, M.C., Boettcher, S.: Real spectra in non-Hermitian Hamiltonians having PT symmetry. Phys. Rev. Lett. **80**, 5243 (1998)
8. Ablowitz, M.J., Musslimani, Z.H.: Integrable nonlocal nonlinear Schrödinger equation. Phys. Rev. Lett. **110**, 064105 (2013)
9. Ablowitz, M.J., Musslimani, Z.H.: Inverse scattering transform for the integrable nonlocal nonlinear Schrödinger equation. Nonlinearity **29**, 915–946 (2016)
10. Yang, J. K.: Nonlinear waves in integrable and nonintegrable systems. Society for Industrial and Applied Mathematics. (2010)
11. Guo, B.L., Liu, N., Wang, Y.: A Riemann-Hilbert approach for a new type coupled nonlinear Schrödinger equations. J. Math. Anal. Appl. **459**(1), 145–158 (2017)
12. Peng, W.Q., Tian, S.F., Wang, X.B., et al.: Riemann-Hilbert method and multi-soliton solutions for three-component coupled nonlinear Schrödinger equations. J. Geom. Phys. **146**, 103508 (2019)
13. Wang, J., Su, T., Geng, X.G.: Riemann-Hilbert approach and N -soliton solutions for a new two-component Sasa-Satsuma equation. Nonlinear Dynam. **101**(1), 597–609 (2020)
14. Zhao, Y., Fan, E.G.: $N$-soliton solution for a higher-order Chen-Lee-Liu equation with nonzero boundary conditions. Mod. Phys. Lett. B **34**(04), 339 (2020)
15. Li, M., Xu, T.: Dark and antidark soliton interactions in the nonlocal nonlinear Schrödinger equation with the self-induced parity-time-symmetric potential. Phys. Rev. E **91**, 033202 (2015)
16. Yan, Z.Y.: Integrable PT-symmetric local and nonlocal vector nonlinear Schrödinger equations: A unified two-parameter model. Appl. Math. Lett. **47**, 61–68 (2015)
17. Yan, Z.Y., Chen, Y., Wen, Z.C.: On stable solitons and interactions of the generalized Gross-Pitaevskii equation with PT-, and non-PT-symmetric potentials. Chaos **26**(8), 5243 (2016)
18. Huang, X., Ling, L.M.: Soliton solutions for the nonlocal nonlinear Schrödinger equation. Eur. Phys. J. Plus **131**(5), 1–11 (2016)
19. Wen, X.Y., Yan, Z.Y., Yang, Y.Q.: Dynamics of higer-order rational solitons for the nonlocal nonlinear Schrödinger equation with the self-induced parity-time-symmetric potential. Chaos **26**, 063123 (2016)
20. Ji, J.L., Zhu, Z.N.: Soliton solutions of an integrable nonlocal modified Korteweg-de Vries equation through inverse scattering transform. J. Math. Anal. Appl. **453**(2), 973–984 (2017)
21. Zhang, H.Q., Tian, B., Li, L.L.: Darboux transformation and soliton solutions for the (2+1)-dimensional nonlinear Schrödinger hierarchy with symbolic computation. Physica A **388**(1), 9–20 (2009)

22. Yang, B., Chen, Y.: Dynamics of rogue waves in the partially pt-symmetric nonlocal Davey-Stewartson systems. Commun. Nonl. Sci. Numer. Simulat. **69**, 287–303 (2019)
23. Yang, J. K.: General $N$-solitons and their dynamics in several nonlocal nonlinear Schrödinger equations. Phys. Lett. A **282** (4) (2019)
24. Lakshmanan, M., Porsezian, K., Daniel, M.: Effect of discreteness on the continuum limit of the Heisenberg spin chain. Phys. Lett. A **133**(9), 483–488 (1988)
25. Christov, I.P.: Enhanced generation of attosecond pulses in dispersion-controlled hollow-core fiber. Phys. Rev. A **60**(4), 3244–3250 (1999)
26. Zhang, X.E., Chen, Y.: Inverse scattering transformation for generalized nonlinear Schrödinger equation. Appl. Math. Lett. **98**, 306–313 (2019)
27. Xu, T., He, G.L.: Higher-order interactional solutions and rogue wave pairs for the coupled Lakshmanan-Porsezian-Daniel equations. Nonlinear. Dyna. **98**(3), 1731–1744 (2019)
28. Chowdury, A., Kedziora, D. J., Ankiewicz, A., et al: Soliton solutions of an integrable nonlinear Schrödinger equation with quintic terms. Phys. Rev. E **90**(3), (2014)
29. Zakharov, V.E., Shabat, A.B.: Integration of the nonlinear equations of mathematical physics by the method of the inverse scattering problem II. Funct. Anal. Appl. **13**, 166–174 (1979)
30. Faddeev, L.D., Takhtadjan, L.A.: Hamiltonian methods in the theory of solitons. Springer, Berlin (1987)
31. Nimmo, J.J.C.: A bilinear B$\ddot{a}$cklund transformation for the nonlinear Schrödinger equation. Phys. Lett. A. **99**, 279–280 (1983)
32. Yang, Y.Q., Yan, Z.Y., Malomed, B.A.: Rogue waves, rational solitons and modulational instability in an integrable fifth-order nonlinear Schrödinger equation. Chaos **25**, 1–11 (2015)
33. Lan, Z.Z., Gao, Y.T., Zhao, C., et al.: Dark soliton interactions for a fifth-order nonlinear Schrodinger equation in a Heisenberg ferromagnetic spin chain. Super. Micro. **100**, 191–197 (2016)
34. Yomba, E., Zakeri, G.A.: Collision of $N$-solitons in a fifth-order nonlinear Schrodinger equation. Wave Motion **72**, 101–112 (2017)
35. Yang, Y.Q., Wang, X., Cheng, X.P.: Higher-order rational solutions for a new integrable nonlocal fifth-order nonlinear Schrödinger equation. Wave Motion **77**, 1–11 (2018)